Transport properties for a Luttinger liquid wire with Rashba spin–orbit coupling and Zeeman splitting

2007 J. Phys.: Condens. Matter 19 136215

(http://iopscience.iop.org/0953-8984/19/13/136215)

IOP PUBLISHING JOURNAL OF PHYSICS: CONDENSED MATTER

J. Phys.: Condens. Matter **19** (2007) 136215 (16pp) doi:10.1088/0953-8984/19/13/136215

Transport properties for a Luttinger liquid wire with Rashba spin–orbit coupling and Zeeman splitting

Fang Cheng[1,2] **and Guanghui Zhou**[1,2,3,4]

[1] CCAST (World Laboratory), PO Box 8730, Beijing 100080, People's Republic of China
[2] Department of Physics, Hunan Normal University, Changsha 410081, People's Republic of China
[3] International Center for Materials Physics, Chinese Academy of Sciences, Shenyang 110015, People's Republic of China

E-mail: ghzhou@hunnu.edu.cn

Received 22 December 2006, in final form 10 February 2007
Published 13 March 2007
Online at stacks.iop.org/JPhysCM/19/136215

Abstract

We study the transport properties for a Luttinger liquid (LL) quantum wire in the presence of both Rashba spin–orbit coupling (SOC) and a weak external in-plane magnetic field. The bosonized Hamiltonian of the system with an externally applied longitudinal electric field is established. Then the equations of motion for the bosonic phase fields are solved in Fourier space, with which both the charge and spin conductivities for the system are calculated analytically, based on linear response theory. Generally, the ac conductivity is an oscillation function of the strengths of electron–electron interaction, Rashba SOC and magnetic field, as well as the driving frequency and the measurement position in the wire. Through analysis with some examples it is demonstrated that the modification of the conductivity due to electron–electron interactions is more remarkable than that due to SOC, while the effects of SOC and Zeeman splitting on the conductivity are very similar. The spin-polarized conductivities for the system in the absence of Zeeman effect or SOC are also discussed. The ratio of the spin-polarized conductivities $\sigma_\uparrow/\sigma_\downarrow$ is dependent on the electron–electron interactions for a system without SOC, while it is independent of the electron–electron interactions for a system without Zeeman splitting.

1. Introduction

The physics of one-dimensional (1D) systems of strongly correlated particles has become a very interesting subject because of the simplicity of the models and the attainment of the truly 1D systems due to breakthroughs in material technology. From the theoretical point of view, the Luttinger liquid (LL) model is appropriate for describing the transport properties of 1D systems

[4] Address for correspondence: Department of Physics, Hunan Normal University, Changsha 410081, People's Republic of China.

with electron–electron interactions [1]. The LL model is of fundamental importance because it is one of very few strongly correlated 'non-Fermi liquid' systems that can be analysed in any detail. The model does not attempt a complete description of electrons in a 1D metal but rather is confined to the vicinity of the Fermi surface. One of the key features of the LL model is the spin-charge separation: the low-energy excitations are not quasiparticles with charge e and spin $\hbar/2$ together but collective modes of spin and charge excitation separately. Therefore, quantum transport in LL systems has attracted a great deal of interest since the experimental realization of the narrow quantum wire formed in semiconductor heterostructures [2] and the carbon nanotube [3], as well as the edge states of the fractional quantum Hall liquid [4]. We will use the first one as our physical subject in this work.

Spintronics is a multidisciplinary field whose central theme is the active manipulation of spin degrees of freedom in solid-state systems. It is believed to be a promising candidate for future information technology [5]. There are two physical mechanisms which can be used to influence the dynamics of the electron spin in normal conductors, i.e., spin–orbit coupling (SOC) and Zeeman splitting. In layered semiconductors devices, the two predominant types of SOC are Dresselhaus SOC [6] and Rashba SOC [7]. The former arises from the breaking of inversion symmetry by the inherent asymmetry of the atomic arrangement in the structure and is not very amenable to external manipulation. The latter, on the other hand, arises from band bending at the interfaces between semiconductor layers and/or any external electric fields applied to the device. Unlike Dresselhaus SOC, the strength of the Rashba SOC can be partially controlled by application of an external electric field perpendicular to the two-dimensional electron gas (2DEG) plane [8]. In many of the proposed spintronics device structures the spin manipulation relies on the Rashba SOC, and as such, only the Rashba SOC will be considered in our work.

In recent few years, there have been tremendous published research works of the SOC effects on the III–V type and II–VI type nonmagnetic semiconductor heterostructures for the purpose of spintronics devices. But there have been only few works [9–15] concerning electron–electron interactions in these spintronic systems. The early theoretical studies [9] demonstrated that the influence of the Zeeman splitting for an LL quantum wire is the breaking of spin-charge separation, where the ratio of the spin-up and spin-down conductivities in a dirty system diverges at low temperatures due to the electron correlation and results in a spin-polarized current. Further studies [10–12] have also shown that the effect of Rashba SOC for the LL wire is that the spin degeneracy is lifted for $k \neq 0$ and each branch loses its vertical symmetry axis, i.e., different directions of motion have different Fermi velocities. Moreover, Coulomb corrections to the extrinsic spin Hall effect of a 2DEG has also been studied recently [13]. In methodology, a bosonization theory including a Rashba SOC [10] or a Zeeman splitting [9] has been constructed. A further question arising naturally is what will happen if both the SOC and Zeeman splitting are considered simultaneously. This motivation has led to the studies [14, 15] on the combined presence of a Rashba SOC and a Zeeman effect in an interacting quantum wire. In these works, the study on a Coulomb long-ranged electron interaction quantum wire [15] in the combined presence of a Rashba SOC and a Zeeman splitting using the perturbative renormalization group treatment has indicated the generation of a spin pseudogap and the propagation of a well-defined spin-oriented current, and on an LL quantum wire [14] by the bosonization technique has demonstrated that the tunnelling current may deviate from a simple power law such as that in an ordinary LL wire.

On the other hand, however, the pure LL quantum wire without SOC and Zeeman splitting has been extensively investigated in the last decade. The ac response of an 1D interacting system has been studied [16–18] previously in the framework of the LL model with or without impurity. Moreover, it is known that the dc limit of conductance through a clean LL quantum

wire is not renormalized by the electron–electron interactions when the reservoirs (leads) are taken into account because of the well-known phenomenon of Andreev-type reflection occurring at the contact between an LL quantum wire and a non-interacting reservoir [19].

In this work, we study the ac dynamical transport properties for a homogenous interacting quantum wire in the presence of both internal Rashba SOC and external magnetic field simultaneously. When a longitudinal time-varying electric field is applied to the wire, in the LL regime we use the bosonization technique and solve the equation of motion for the system in Fourier space. It is found that in this case the spin and charge degrees of freedom are completely coupled and can be characterized by four new different velocities. Within the linear response theory, the dynamical ac ($\omega \neq 0$) conductivity of the system is generally an oscillation function of the strengths of electron–electron interaction, Rashba SOC and Zeeman interaction as well as the driving frequency and the measurement position in the wire. However, the modification of the conductivity due to electron–electron interactions is more remarkable than that due to SOC, while the effects of SOC and Zeeman splitting on the conductivity are very similar. The spin-polarized conductivities for the system in the absence of Zeeman effect or SOC are also discussed. The ratio of the spin-polarized conductivities $\sigma_\uparrow/\sigma_\downarrow$ is dependent on the electron–electron interactions for the system without SOC, and the ratio becomes more different when the electron–electron interactions are stronger, while it is independent of the electron–electron interactions for the system without Zeeman splitting. To the best of our knowledge, some of these phenomena have not been reported previously for the LL quantum wire system.

The rest of the paper is organized as follows. In section 2, we formulate the model Hamiltonian in the bosonization form for an interacting quantum wire simultaneously with an external longitudinal electric field applied and both Rashba SOC and Zeeman splitting, and solve the equation of motion for the bosonic phase fields in Fourier space. Within the linear response theory, the conductivity of the system is analytically calculated in section 3, and the detailed results for the two limited cases without either Zeeman splitting or Rashba SOC are demonstrated in two subsections, respectively. Some examples and the discussion of the results are demonstrated in section 4. Finally, section 5 concludes the paper.

2. The Hamiltonian and bosonization

Consider the system consisting of an interacting 1D quantum wire with an applied longitudinal electric field induced realized by an externally applied electromagnetic radiation in the experiments. Assume that we have a system of length L with a boundary condition. In the 1D quantum wire the electron is subjected to a Rashba SOC. Here we have taken the symmetric centre of the quantum wire as the origin, and the growth direction of the heterostructure to be the z-axis in our spatial coordinate system. The electron transport ballistically in the quantum wire is along the longitudinal x-direction. A magnetic field B perpendicular to the quantum wire is applied along the y-axis.

For a weak magnetic field, its coupling to the electron orbital can be neglected [14] if the low-lying excitation is considered, so we only keep the Zeeman Hamiltonian term with respect to the magnetic field. Assuming $\delta v_{\mathrm{R}} \sim \delta v_{\mathrm{B}} \ll v_{\mathrm{F}}$, the linearized noninteracting electron Hamiltonian of the quantum wire with both Rashba SOC and Zeeman splitting is given by [9, 10, 14]

$$H_0 = -\mathrm{i}\hbar \int \sum_{\gamma,s} v_\gamma^s \psi_{\gamma s}^+ \partial_x \psi_{\gamma s}\, \mathrm{d}x. \tag{1}$$

The operators $\psi_{\gamma s}$ ($\gamma = \mathrm{L}, \mathrm{R}$; $s = \downarrow, \uparrow$) annihilate spin-down ($\downarrow$) and spin-up ($\uparrow$) electrons near the left (L) and right (R) Fermi points. In what follows, the indices γ and s take the values

-1 (1) for L (R) and $\downarrow$ ($\uparrow$), respectively. And $v_\gamma^s = \gamma v_\mathrm{F} - \frac{1}{2}s\delta v_\mathrm{R} + \frac{1}{2}\gamma s\delta v_\mathrm{B}$ are four different sound velocities. Here v_F is the bare Fermi velocity of noninteracting right and left movers, $\delta v_\mathrm{R} = 2\alpha/\hbar$ (α is the strength of Rashba SOC) and $\delta v_\mathrm{B} = g'\mu_\mathrm{B}B/k_F$ (B is the magnitude of magnetic field, g' is the Lande factor, and μ_B is the Bohr magneton, respectively). Equation (1) shows clearly that the Rashba term splits the bands horizontally and makes the electron Fermi velocities become different for different directions of motion, while the Zeeman term splits the bands vertically and makes the electron Fermi velocities become different for different directions of spin. Using the bosonization technique [20] in terms of

$$\psi_{\gamma s}^{+}\partial_x\psi_{\gamma s} = \mathrm{i}\gamma\left(\frac{\gamma\partial_x\vartheta_s - \frac{\Pi_s}{\hbar}}{2}\right)^2, \tag{2}$$

we can derive the Hamiltonian (1) as

$$\begin{aligned} H_0 = {} & \frac{\hbar v_\mathrm{F}}{2}\int \mathrm{d}x\left[(\partial_x\vartheta_\uparrow)^2 + \left(\frac{\Pi_\uparrow}{\hbar}\right)^2 + (\partial_x\vartheta_\downarrow)^2 + \left(\frac{\Pi_\downarrow}{\hbar}\right)^2\right] \\ & - \frac{\hbar}{2}\delta v_\mathrm{B}\int \mathrm{d}x\left[(\partial_x\vartheta_\downarrow)^2 + \left(\frac{\Pi_\downarrow}{\hbar}\right)^2 - (\partial_x\vartheta_\uparrow)^2 - \left(\frac{\Pi_\uparrow}{\hbar}\right)^2\right] \\ & + \frac{\delta v_\mathrm{R}}{2}\int \mathrm{d}x\,[\Pi_\uparrow(\partial_x\vartheta_\uparrow) - \Pi_\downarrow(\partial_x\vartheta_\downarrow)], \end{aligned} \tag{3}$$

where $\vartheta_{\uparrow/\downarrow}$ is the phase field for spin-up/down electrons and $\Pi_{\uparrow/\downarrow}$ is the corresponding conjugate momentum. With the transformation

$$\vartheta_\rho = \frac{\vartheta_\uparrow + \vartheta_\downarrow}{\sqrt{2}}, \qquad \vartheta_\sigma = \frac{\vartheta_\uparrow - \vartheta_\downarrow}{\sqrt{2}}, \qquad \Pi_\rho = \frac{\Pi_\uparrow + \Pi_\downarrow}{\sqrt{2}}, \qquad \Pi_\sigma = \frac{\Pi_\uparrow - \Pi_\downarrow}{\sqrt{2}}, \tag{4}$$

we can reduce equation (3) into

$$\begin{aligned} H_0 = {} & \frac{\hbar v_\mathrm{F}}{2}\int \mathrm{d}x\left[(\partial_x\vartheta_\rho)^2 + \left(\frac{\Pi_\rho}{\hbar}\right)^2 + (\partial_x\vartheta_\sigma)^2 + \left(\frac{\Pi_\sigma}{\hbar}\right)^2\right] \\ & + \frac{\hbar}{2}\delta v_\mathrm{B}\int \mathrm{d}x\left[(\partial_x\vartheta_\sigma)(\partial_x\vartheta_\rho) + \frac{1}{\hbar^2}\Pi_\rho\Pi_\sigma\right] \\ & + \frac{\delta v_\mathrm{R}}{2}\int \mathrm{d}x\,[\Pi_\sigma(\partial_x\vartheta_\rho) + \Pi_\rho(\partial_x\vartheta_\sigma)], \end{aligned} \tag{5}$$

where ϑ_ρ and ϑ_σ can be considered as the phase field corresponding to the charge degree and the spin degree of freedom, respectively, and Π_ρ and Π_σ are the corresponding conjugate momenta.

Next, the short-ranged electron–electron interactions in the wire give a term to the Hamiltonian

$$H_\mathrm{int} = \frac{V(q=0)}{2\pi}\int \mathrm{d}x\,(\partial_x\vartheta_\rho)^2, \tag{6}$$

where $V(q=0)$ is the electron–electron interaction potential. In this Hamiltonian we have neglected the Umklapp scattering, which is not relevant in the quantum wires formed in a semiconductor heterostructure.

Finally, we consider the Hamiltonian term of a longitudinal electric field applied to the quantum wire. We use the method of describing the application of an external bias voltage [19]. With the electron charge $-e$, the coupling to an external time-dependent potential $U_\mathrm{R}(t)$ yields a term in the Hamiltonian as [17]

$$H_\mathrm{ac} = -e\int \mathrm{d}x\,\rho(x)U_\mathrm{R}(x,t) = \sqrt{\frac{2}{\pi}}e\int \mathrm{d}x\,\partial_x U_\mathrm{R}(x,t)\vartheta_\rho, \tag{7}$$

where $U_{\mathrm{R}}(x,t)$ is the chemical potential of the right-moving electrons, and $\rho(x,t) = \sqrt{\frac{2}{\pi}}\partial_x\vartheta_\rho(x,t)$ is the charge density in bosonization presentation. By virtue of the relation $\partial_x U_{\mathrm{R}}(x,t) = -E(x,t)$, equation (7) can be expressed as

$$H_{\mathrm{ac}} = -\sqrt{\frac{2}{\pi}}e\int \mathrm{d}x\, E(x,t)\vartheta_\rho(x,t), \tag{8}$$

where $E(x,t)$ is the externally applied electric field.

Combining equations (5), (6) and (8), we finally obtain the total bosonized Hamiltonian for the system:

$$\begin{aligned} H = {} & \frac{\hbar}{2}\int \mathrm{d}x\left[\frac{v_\rho}{g}(\partial_x\vartheta_\rho)^2 + v_{\mathrm{F}}\left(\frac{\Pi_\rho}{\hbar}\right)^2\right] + \frac{\hbar}{2}\int \mathrm{d}x\left[v_\sigma(\partial_x\vartheta_\sigma)^2 + v_\sigma\left(\frac{\Pi_\sigma}{\hbar}\right)^2\right] \\ & + \frac{\hbar}{2}\delta v_{\mathrm{B}}\int \mathrm{d}x\left[(\partial_x\vartheta_\sigma)(\partial_x\vartheta_\rho) + \frac{1}{\hbar^2}(\Pi_\rho\Pi_\sigma)\right] \\ & + \frac{\hbar}{2}\delta v_{\mathrm{R}}\int \mathrm{d}x\left[\left(\frac{\Pi_\sigma}{\hbar}\right)(\partial_x\vartheta_\rho) + \left(\frac{\Pi_\rho}{\hbar}\right)(\partial_x\vartheta_\sigma)\right] \\ & - \sqrt{\frac{2}{\pi}}e\int \mathrm{d}x\, E(x,t)\vartheta_\rho(x,t), \end{aligned} \tag{9}$$

where $v_{\rho,\sigma}$ are the propagation velocities of the charge and spin collective modes of the decoupled model ($\delta v_{\mathrm{B}} = \delta v_{\mathrm{R}} = 0$, or $B = \alpha = 0$) and the parameter g is the strength of the electron–electron interactions, which is defined as $1/g^2 = 1 + V(q=0)/\hbar\pi v_{\mathrm{F}}$ with v_{F} the non-interacting fermion velocity of the system; non-interacting fermions corresponds to $g = 1$ and repulsive interaction corresponds to $g < 1$. The velocities $v_{\rho,\sigma}$ have been obtained as function of g and v_{F} in [20] as $v_\rho = v_{\mathrm{F}}/g$ and $v_\sigma = v_{\mathrm{F}}$ for the decoupled model.

Further, the action functional of the coupled system can be written in terms of the phase fields $\vartheta_\rho(x,t)$ and $\vartheta_\sigma(x,t)$ as

$$\begin{aligned} S = {} & \frac{\hbar}{2}\int \mathrm{d}t\int \mathrm{d}x\left[\frac{1}{gv_\rho}(\partial_t\vartheta_\rho)^2 - \frac{v_\rho}{g}(\partial_x\vartheta_\rho)^2\right] + \frac{\hbar}{2}\int \mathrm{d}t\int \mathrm{d}x\left[\frac{1}{v_\sigma}(\partial_t\vartheta_\sigma)^2 - v_\sigma(\partial_x\vartheta_\sigma)^2\right] \\ & - \frac{\hbar}{2}\delta v_{\mathrm{B}}\int \mathrm{d}x\left[(\partial_x\vartheta_\sigma)(\partial_x\vartheta_\rho) + \frac{1}{(v_{\mathrm{F}})^2}(\partial_t\vartheta_\rho)(\partial_t\vartheta_\sigma)\right] \\ & - \frac{\hbar}{2}\frac{\delta v_{\mathrm{R}}}{v_{\mathrm{F}}}\int \mathrm{d}t\int \mathrm{d}x[(\partial_t\vartheta_\sigma)(\partial_x\vartheta_\rho) + (\partial_t\vartheta_\rho)(\partial_x\vartheta_\sigma)] \\ & + \sqrt{\frac{2}{\pi}}e\int \mathrm{d}x\, E(x,t)\vartheta_\rho(x,t). \end{aligned} \tag{10}$$

Note that in our system the time derivative of the field is not proportional to the conjugate canonical momentum, but is a linear combination of the canonical momentum (including charge canonical momenta and spin canonical momenta) and the gradient of the field. However, after omitting the second order of the shifts from the spin–orbit or the Zeeman term and the product between them, we find that the extra charge or spin canonical momentum and the gradient of the field produce the same terms in the first line of equation (9), and the first term $(\Pi_\rho\partial_t\vartheta_\rho + \Pi_\sigma\partial_t\vartheta_\sigma)$ of the Lagrangian $L = \int \mathrm{d}x\,(\Pi_\rho\partial_t\vartheta_\rho + \Pi_\sigma\partial_t\vartheta_\sigma) - H$, which finally mean that the extra charge or spin canonical momentum and the gradient of the field do not have an effect on the action functional of the coupled system. Therefore, by minimizing the action (10) we obtain its associated equations of motion for the phase fields:

$$\frac{\hbar}{gv_\rho}\partial_t^2\vartheta_\rho - \frac{\hbar v_\rho}{g}\partial_x^2\vartheta_\rho - \hbar\frac{\delta v_{\mathrm{R}}}{v_{\mathrm{F}}}\partial_t\partial_x\vartheta_\sigma - \frac{\hbar}{2}\delta v_{\mathrm{B}}\partial_x^2\vartheta_\sigma - \frac{\hbar}{2}\frac{\delta v_{\mathrm{B}}}{{v_{\mathrm{F}}}^2}\partial_t^2\vartheta_\sigma + \sqrt{\frac{2}{\pi}}eE(x,t) = 0, \tag{11}$$

$$\frac{\hbar}{v_\sigma}\partial_t^2\vartheta_\sigma - \hbar v_\sigma \partial_x^2\vartheta_\sigma - \hbar\frac{\delta v_\mathrm{R}}{v_\mathrm{F}}\partial_t\partial_x\vartheta_\rho - \frac{\hbar}{2}\delta v_\mathrm{B}\partial_x^2\vartheta_\rho - \frac{\hbar}{2}\frac{\delta v_\mathrm{B}}{{v_\mathrm{F}}^2}\partial_t^2\vartheta_\rho = 0. \tag{12}$$

Applying the Fourier transformation

$$\vartheta(x,t) = \frac{1}{(2\pi)^2}\int \mathrm{d}q \int \mathrm{d}\omega\, \vartheta(q,\omega)\mathrm{e}^{-\mathrm{i}qx+\mathrm{i}\omega t} \tag{13}$$

to equations (11) and (12), we have the solution for the phase fields:

$$\vartheta_\rho(q,\omega) = \sqrt{\frac{2}{\pi}}\frac{ev_\mathrm{F}}{\hbar}\frac{E(q,\omega)}{(\omega^2 - v_\rho^2 q^2) - \frac{(\delta v_\mathrm{R} q\omega - \frac{1}{2}\delta v_\mathrm{B} v_\mathrm{F} q^2 - \frac{1}{2}\frac{\delta v_\mathrm{B}}{v_\mathrm{F}}\omega^2)^2}{\omega^2 - v_\sigma^2 q^2}}, \tag{14}$$

$$\vartheta_\sigma(q,\omega) = -\sqrt{\frac{2}{\pi}}\frac{ev_\mathrm{F}}{\hbar}\frac{(\delta v_\mathrm{R} q\omega - \frac{1}{2}\delta v_\mathrm{B} v_\mathrm{F} q^2 - \frac{1}{2}\frac{\delta v_\mathrm{B}}{v_\mathrm{F}}\omega^2)E(q,\omega)}{(\omega^2 - v_\rho^2 q^2)(\omega^2 - v_\sigma^2 q^2) - (\delta v_\mathrm{R} q\omega - \frac{1}{2}\delta v_\mathrm{B} v_\mathrm{F} q^2 - \frac{1}{2}\frac{\delta v_\mathrm{B}}{v_\mathrm{F}}\omega^2)^2}. \tag{15}$$

3. Conductivity of the system

The current operator can be defined by using the 1D continuity equation $\partial_x j_\rho(x,t) = e\partial_t\rho(x,t)$. Then we have the charge current

$$j_\rho(x,t) = \sqrt{\frac{2}{\pi}}e\partial_t\vartheta_\rho(x,t). \tag{16}$$

Therefore, using solution (14) for $\vartheta_\rho(q,\omega)$, we obtain the explicit expression for the charge current operator:

$$j_\rho(q,\omega) = \frac{\mathrm{i}e^2 v_\mathrm{F}}{\hbar\pi}\frac{2\omega(\omega^2 - v_\sigma^2 q^2)E(q,\omega)}{(\omega^2 - v_\rho^2 q^2)(\omega^2 - v_\sigma^2 q^2) - (\delta v_\mathrm{R} q\omega - \frac{1}{2}\delta v_\mathrm{B} v_\mathrm{F} q^2 - \frac{1}{2}\frac{\delta v_\mathrm{B}}{v_\mathrm{F}}\omega^2)^2}. \tag{17}$$

The charge current operator is written further as

$$j_\rho(q,\omega) = \frac{\mathrm{i}e^2 v_\mathrm{F}}{\hbar\pi}\frac{\mathrm{i}E(q,\omega)}{1 - \dfrac{\delta v_\mathrm{B}^2}{4v_\mathrm{F}^2}}\frac{2\omega(\omega^2 - v_\sigma^2 q^2)}{(\omega + u_1 q)(\omega + u_2 q)(\omega + u_3 q)(\omega + u_4 q)}, \tag{18}$$

where $u_{1,2,3,4}$ are the velocities of four independent branches of the chiral excitations, and they are all related to g, δv_R and δv_B [14]. Since the linear response is exact for an ideal LL, the external electric field has to be used for the conductivity calculation [18], i.e.,

$$j_\rho(q,\omega) = \sigma(q,\omega)E(q,\omega). \tag{19}$$

Therefore, combining equation (17) with (19), we obtain the nonlocal charge conductivity:

$$\sigma_\rho(q,\omega) = \frac{\mathrm{i}e^2 v_\mathrm{F}}{\hbar\pi}\frac{2\omega(\omega^2 - v_\sigma^2 q^2)}{(\omega^2 - v_\rho^2 q^2)(\omega^2 - v_\sigma^2 q^2) - (\delta v_\mathrm{R} q\omega - \frac{1}{2}\delta v_\mathrm{B} v_\mathrm{F} q^2 - \frac{1}{2}\frac{\delta v_\mathrm{B}}{v_\mathrm{F}}\omega^2)^2}. \tag{20}$$

On the other hand, the bosonic phase field ϑ_σ is related to the spin current operator through

$$j_\sigma = \sqrt{\frac{2}{\pi}}e\partial_t\vartheta_\sigma. \tag{21}$$

Combing equations (15) and (21), the spin current operator can be expressed as

$$j_\sigma(q,\omega) = \frac{\mathrm{i}e^2 v_\mathrm{F}}{\hbar\pi}\frac{2\omega(\delta v_\mathrm{R} q\omega - \frac{1}{2}\delta v_\mathrm{B} v_\mathrm{F} q^2 - \frac{1}{2}\frac{\delta v_\mathrm{B}}{v_\mathrm{F}}\omega^2)E(q,\omega)}{(\omega^2 - v_\rho^2 q^2)(\omega^2 - v_\sigma^2 q^2) - (\delta v_\mathrm{R} q\omega - \frac{1}{2}\delta v_\mathrm{B} v_\mathrm{F} q^2 - \frac{1}{2}\frac{\delta v_\mathrm{B}}{v_\mathrm{F}}\omega^2)^2}. \tag{22}$$

Therefore, using the linear response relation (19), we can also obtain the spin conductivity:

$$\sigma_\sigma(q,\omega) = \frac{\mathrm{i}e^2 v_\mathrm{F}}{\hbar\pi} \frac{2\omega(\delta v_\mathrm{R} q\omega - \frac{1}{2}\delta v_\mathrm{B} v_\mathrm{F} q^2 - \frac{1}{2}\frac{\delta v_\mathrm{B}}{v_\mathrm{F}}\omega^2)}{(\omega^2 - v_\rho^2 q^2)(\omega^2 - v_\sigma^2 q^2) - (\delta v_\mathrm{R} q\omega - \frac{1}{2}\delta v_\mathrm{B} v_\mathrm{F} q^2 - \frac{1}{2}\frac{\delta v_\mathrm{B}}{v_\mathrm{F}}\omega^2)^2} \tag{23}$$

which is also a function of g, α, B, ω and q.

Next, for understanding the transport property of the system in more detail, we go further for the two limited cases of $B = 0$ or $\alpha = 0$, respectively, in the following subsections.

3.1. The conductivity with Rashba SOC

Consider an LL quantum wire submitted to Rashba SOC without a Zeeman splitting, i.e., in the absence of external magnetic field ($B = 0$ or $\delta v_\mathrm{B} = 0$). In this case the expression of the current operator equation (17) is reduced to

$$j_\rho(q,\omega) = \frac{\mathrm{i}e^2 v_\mathrm{F}}{\hbar\pi} \frac{2\omega(\omega^2 - v_\sigma^2 q^2)E(q,\omega)}{(\omega^2 - u_1^2 q^2)(\omega^2 - u_2^2 q^2)}, \tag{24}$$

where

$$u_{1,2}^2 = \frac{\delta v_\mathrm{R}^2 + v_\rho^2 + v_\sigma^2}{2} \pm \frac{\sqrt{(\delta v_\mathrm{R}^2 + v_\rho^2 + v_\sigma^2)^2 - 4v_\rho^2 v_\sigma^2}}{2} \tag{25}$$

are the propagation velocities of coupled collective modes in which the subscript $1/2$ corresponds to $+/-$. Furthermore, in the absence of SOC ($\alpha = 0$ or $\delta v_\mathrm{R} = 0$), we simply have $u_{1,2} = v_{\rho,\sigma}$ which correspond to the velocities for the special case of spin-charge separation in an LL quantum wire [16]. Moreover, equation (24) can be rewritten as

$$\begin{aligned} j_\rho(q,\omega) = \frac{\mathrm{i}e^2 v_\mathrm{F} E(q,\omega)}{\hbar\pi} \Bigg[& \frac{u_1^2 - v_\sigma^2}{u_1^2 - u_2^2}\left(\frac{1}{\omega + u_1 q} + \frac{1}{\omega - u_1 q}\right) \\ & - \frac{u_2^2 - v_\sigma^2}{u_1^2 - u_2^2}\left(\frac{1}{\omega + u_2 q} + \frac{1}{\omega - u_2 q}\right)\Bigg]. \end{aligned} \tag{26}$$

Therefore, combining equation (19) with (26), we obtain the nonlocal charge conductivity:

$$\sigma_\rho(q,\omega) = \frac{\mathrm{i}e^2 v_\mathrm{F}}{\hbar\pi}\left[\frac{u_1^2 - v_\sigma^2}{u_1^2 - u_2^2}\left(\frac{1}{\omega + u_1 q} + \frac{1}{\omega - u_1 q}\right) - \frac{u_2^2 - v_\sigma^2}{u_1^2 - u_2^2}\left(\frac{1}{\omega + u_2 q} + \frac{1}{\omega - u_2 q}\right)\right], \tag{27}$$

which can be transformed into real space:

$$\sigma_\rho(x,\omega) = \frac{2e^2}{h}\left[\frac{(u_1^2 - v_\sigma^2)v_\mathrm{F}}{(u_1^2 - u_2^2)u_1} \mathrm{e}^{\mathrm{i}\frac{\omega}{u_1}|x|} - \frac{(u_2^2 - v_\sigma^2)v_\mathrm{F}}{(u_1^2 - u_2^2)u_2} \mathrm{e}^{\mathrm{i}\frac{\omega}{u_2}|x|}\right]. \tag{28}$$

For convenience we use the abbreviation $\xi = x/l$, in which ξ provides a dimensionless measured position in the wire and l is the unit of length. Hence, equation (28) is reduced to

$$\sigma_\rho(x,\omega) = \frac{2e^2}{h}\left[\frac{(u_1^2 - v_\sigma^2)v_\mathrm{F}}{(u_1^2 - u_2^2)u_1} \mathrm{e}^{\mathrm{i}\frac{\omega l}{u_1}|\xi|} - \frac{(u_2^2 - v_\sigma^2)v_\mathrm{F}}{(u_1^2 - u_2^2)u_2} \mathrm{e}^{\mathrm{i}\frac{\omega l}{u_2}|\xi|}\right]. \tag{29}$$

This result implicates that the ac charge conductivity of a perfect LL quantum wire with Rashba SOC is an oscillation function of the interaction parameter, SOC strength and the driving

frequency as well as the measurement position in the wire. And in the limit of vanishing spin–orbit and Zeeman coupling, the dc charge conductivity $\sigma_\rho = 2ge^2/h$, which is in agreement with the conductivity found in previous studies [18].

In addition, in the case of an LL wire with Rashba SOC only, equation (22) for the spin current operator is reduced to

$$j_\sigma(q,\omega) = \frac{\mathrm{i}e^2 v_\mathrm{F}}{\hbar\pi}\frac{2\omega(-\delta v_\mathrm{R} q\omega)E(q,\omega)}{(\omega^2-u_1^2q^2)(\omega^2-u_2^2q^2)}, \tag{30}$$

and a similar calculation leads to the nonlocal spin conductivity for the system:

$$\sigma_\sigma(x,\omega) = \frac{2e^2}{h}\frac{\delta v_\mathrm{R} v_\mathrm{F}}{u_1^2-u_2^2}\mathrm{sgn}(\xi)\left(\mathrm{e}^{\mathrm{i}\frac{\omega l}{u_1}|\xi|}-\mathrm{e}^{\mathrm{i}\frac{\omega l}{u_2}|\xi|}\right), \tag{31}$$

where $\mathrm{sgn}(\xi) = -1$ for $\xi < 0$ and 1 for $\xi > 0$. This expression for spin conductivity has a less complicated dependence on the system parameters than that for charge conductivity (29). However, the spin conductivity vanishes as $\delta v_\mathrm{R} = 0$ or $\omega = 0$.

Furthermore, if we reverse the transformation (4) and define the total (charge) conductivity $\sigma_\rho = \sigma_\uparrow + \sigma_\downarrow$ and the difference (spin) conductivity $\sigma_\sigma = \sigma_\uparrow - \sigma_\downarrow$, then the combination of equations (29) and (31) gives

$$\begin{aligned}\sigma_\uparrow = \frac{e^2}{h}\Bigg[&\left(\frac{(u_1^2-v_\sigma^2)v_\mathrm{F}}{(u_1^2-u_2^2)u_1}+\frac{\delta v_\mathrm{R} v_\mathrm{F}}{u_1^2-u_2^2}\mathrm{sgn}(\xi)\right)\mathrm{e}^{\mathrm{i}\frac{\omega l}{u_1}|\xi|}\\ &-\left(\frac{(u_2^2-v_\sigma^2)v_\mathrm{F}}{(u_1^2-u_2^2)u_2}+\frac{\delta v_\mathrm{R} v_\mathrm{F}}{u_1^2-u_2^2}\mathrm{sgn}(\xi)\right)\mathrm{e}^{\mathrm{i}\frac{\omega l}{u_2}|\xi|}\Bigg]\\ &\overset{\omega\to 0}{=\!=} \frac{e^2}{h}\frac{v_\mathrm{F}}{u_1^2-u_2^2}\left(\frac{u_1^2-v_\sigma^2}{u_1}-\frac{u_2^2-v_\sigma^2}{u_2}\right)\end{aligned} \tag{32}$$

and

$$\begin{aligned}\sigma_\downarrow = \frac{e^2}{h}\Bigg[&\left(\frac{(u_1^2-v_\sigma^2)v_\mathrm{F}}{(u_1^2-u_2^2)u_1}-\frac{\delta v_\mathrm{R} v_\mathrm{F}}{u_1^2-u_2^2}\mathrm{sgn}(\xi)\right)\mathrm{e}^{\mathrm{i}\frac{\omega l}{u_1}|\xi|}\\ &-\left(\frac{(u_2^2-v_\sigma^2)v_\mathrm{F}}{(u_1^2-u_2^2)u_2}-\frac{\delta v_\mathrm{R} v_\mathrm{F}}{u_1^2-u_2^2}\mathrm{sgn}(\xi)\right)\mathrm{e}^{\mathrm{i}\frac{\omega l}{u_2}|\xi|}\Bigg]\\ &\overset{\omega\to 0}{=\!=} \frac{e^2}{h}\frac{v_\mathrm{F}}{u_1^2-u_2^2}\left(\frac{u_1^2-v_\sigma^2}{u_1}-\frac{u_2^2-v_\sigma^2}{u_2}\right)\end{aligned} \tag{33}$$

for the conductivity of spin-up and spin-down electrons, respectively. From equations (32) and (33), we can see that in the case of $\omega = 0$ or without Rashba SOC ($\delta v_\mathrm{R} = 0$), the conductivities for the two spin subbands are degenerate. Defining $v_{\mathrm{F}\uparrow} = v_\mathrm{F} - \delta v_\mathrm{R}/2$ ($v_{\mathrm{F}\downarrow} = v_\mathrm{F} + \delta v_\mathrm{R}/2$) as the Fermi velocity of the spin-up (spin-down) subband in the presence of Rashba SOC, we can express $\delta v_\mathrm{R}/v_\mathrm{F}$ as

$$\frac{\delta v_\mathrm{R}}{v_\mathrm{F}} = \frac{2(\frac{v_{\mathrm{F}\downarrow}}{v_{\mathrm{F}\uparrow}}-1)}{\frac{v_{\mathrm{F}\downarrow}}{v_{\mathrm{F}\uparrow}}+1}, \tag{34}$$

in which $v_{\mathrm{F}\uparrow} = v_{\mathrm{F}\downarrow}$ when $\delta v_\mathrm{R} = 0$.

3.2. The conductivity with Zeeman splitting

In this subsection we consider the case of the system with Zeeman splitting in the absence of SOC, i.e., in the case of $\alpha = 0$ or $\delta v_\mathrm{R} = 0$. In this case the charge current operator reads

$$j_\rho(q,\omega) = \frac{\mathrm{i}e^2 v_\mathrm{F}}{\hbar\pi}\frac{2\omega(\omega^2-v_\sigma^2q^2)E(q,\omega)}{[1-(\frac{\delta v_\mathrm{R}}{2v_\mathrm{F}})^2](\omega^2-u_1^2q^2)(\omega^2-u_2^2q^2)}, \tag{35}$$

where

$$u_{1,2}^2 = \frac{v_\rho^2 + v_\sigma^2 + \frac{\delta v_B^2}{2}}{2[1-(\frac{\delta v_B}{2v_F})^2]} \pm \sqrt{\left(\frac{v_\rho^2 + v_\sigma^2 + \frac{\delta v_B^2}{2}}{2[1-(\frac{\delta v_B}{2v_F})^2]}\right)^2 - \frac{v_\rho^2 v_\sigma^2 - \frac{\delta v_B^2 v_F^2}{4}}{1-(\frac{\delta v_B}{2v_F})^2}} \tag{36}$$

are the propagation velocities of collective modes. Again, when $\delta v_B = 0$, they are also reduced to the velocities for the spin-charge separated system $u_{1,2} = v_{\rho,\sigma}$ [16, 19].

Additionally, through the same procedures as above, we obtain the result for the nonlocal charge conductivity:

$$\sigma_\rho(q,\omega) = \frac{ie^2 v_F}{\hbar\pi}\frac{1}{1-(\frac{\delta v_B}{2v_F})^2}\left[\frac{u_1^2 - v_\sigma^2}{u_1^2 - u_2^2}\left(\frac{1}{\omega + u_1 q} + \frac{1}{\omega - u_1 q}\right)\right.$$
$$\left. - \frac{u_2^2 - v_\sigma^2}{u_1^2 - u_2^2}\left(\frac{1}{\omega + u_2 q} + \frac{1}{\omega - u_2 q}\right)\right], \tag{37}$$

which can be transformed into real space:

$$\sigma_\rho(x,\omega) = \frac{2e^2}{h}\frac{1}{1-(\frac{\delta v_B}{2v_F})^2}\left[\frac{(u_1^2 - v_\sigma^2)v_F}{(u_1^2 - u_2^2)u_1}e^{i\frac{\omega l}{u_1}|\xi|} - \frac{(u_2^2 - v_\sigma^2)v_F}{(u_1^2 - u_2^2)u_2}e^{i\frac{\omega l}{u_2}|\xi|}\right]. \tag{38}$$

From this expression we can see that the ac conductivity of a perfect LL with only Zeeman splitting is also an oscillation function of the interaction parameter, magnetic field intensity and the driving frequency as well as the measurement position in the wire.

Accordingly, using the same method as above, the spin conductivity for the LL wire with only Zeeman splitting is obtained as

$$\sigma_\sigma(x,\omega) = \frac{2e^2}{h}\frac{\frac{\delta v_B}{2v_F}}{1-(\frac{\delta v_B}{2v_F})^2}\left[\frac{(u_1^2 + v_F^2)v_F}{(u_1^2 - u_2^2)u_1}e^{i\frac{\omega l}{u_1}|\xi|} - \frac{(u_2^2 + v_F^2)v_F}{(u_1^2 - u_2^2)u_2}e^{i\frac{\omega l}{u_2}|\xi|}\right]. \tag{39}$$

We also see that as $\delta v_B = 0$, the spin conductivity vanishes. Under the same definition of the total (charge) conductivity $\sigma_\rho = \sigma_\uparrow + \sigma_\downarrow$ and the difference (spin) conductivity $\sigma_\sigma = \sigma_\uparrow - \sigma_\downarrow$ with the combination of equations (38) and (39), we can obtain

$$\sigma_\uparrow = \frac{e^2}{h}\frac{1}{1-(\frac{\delta v_B}{2v_F})^2}\frac{v_F}{u_1^2 - u_2^2}\left[\left(\frac{u_1^2 - v_\sigma^2}{u_1} + \frac{\delta v_B}{2v_F}\frac{u_1^2 + v_F^2}{u_1}\right)e^{i\frac{\omega l}{u_1}|\xi|}\right.$$
$$\left. - \left(\frac{u_2^2 - v_\sigma^2}{u_2} + \frac{\delta v_B}{2v_F}\frac{u_2^2 + v_F^2}{u_2}\right)e^{i\frac{\omega l}{u_2}|\xi|}\right]$$
$$\overset{\omega\to 0}{=\!=} \frac{e^2}{h}\frac{1}{1-(\frac{\delta v_B}{2v_F})^2}\frac{v_F}{u_1^2 - u_2^2}\left[\left(\frac{u_1^2 - v_\sigma^2}{u_1} + \frac{\delta v_B}{2v_F}\frac{u_1^2 + v_F^2}{u_1}\right)\right.$$
$$\left. - \left(\frac{u_2^2 - v_\sigma^2}{u_2} + \frac{\delta v_B}{2v_F}\frac{u_2^2 + v_F^2}{u_2}\right)\right] \tag{40}$$

and

$$\sigma_\downarrow = \frac{e^2}{h}\frac{1}{1-(\frac{\delta v_B}{2v_F})^2}\frac{v_F}{u_1^2 - u_2^2}\left[\left(\frac{u_1^2 - v_\sigma^2}{u_1} - \frac{\delta v_B}{2v_F}\frac{u_1^2 + v_F^2}{u_1}\right)e^{i\frac{\omega l}{u_1}|\xi|}\right.$$
$$\left. - \left(\frac{u_2^2 - v_\sigma^2}{u_2} - \frac{\delta v_B}{2v_F}\frac{u_2^2 + v_F^2}{u_2}\right)e^{i\frac{\omega l}{u_2}|\xi|}\right]$$

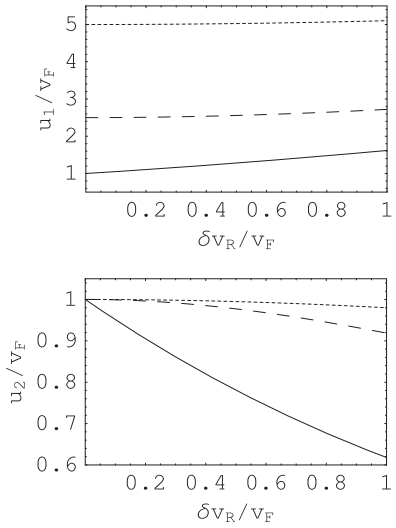

Figure 1. The plotted propagation velocities of the collective modes $u_{1,2}$ (in units of v_F) as a function of the SOC strength $\delta v_R/v_F$ in the absence of Zeeman effect, where the solid lines for $g = 1$, the dashed lines for $g = 0.4$ and the dotted lines for $g = 0.2$, respectively.

$$\overset{\omega\to 0}{=\!=} \frac{e^2}{h}\frac{1}{1-(\frac{\delta v_B}{2v_F})^2}\frac{v_F}{u_1^2-u_2^2}\left[\left(\frac{u_1^2-v_\sigma^2}{u_1}-\frac{\delta v_B}{2v_F}\frac{u_1^2+v_F^2}{u_1}\right)\right.$$
$$\left.-\left(\frac{u_2^2-v_\sigma^2}{u_2}-\frac{\delta v_B}{2v_F}\frac{u_2^2+v_F^2}{u_2}\right)\right] \tag{41}$$

for the conductivities of spin-up and spin-down electrons, respectively. We also see that without Zeeman splitting ($\delta v_B = 0$) the conductivities for the two spin subbands are degenerate. Again, defining $v_{F\uparrow} = v_F + \delta v_B/2$ ($v_{F\downarrow} = v_F - \delta v_B/2$) as the Fermi velocity of the up (down) spin subband in a magnetic field B, we can also express $\delta v_B/v_F$ as

$$\frac{\delta v_B}{v_F} = \frac{2(\frac{v_{F\uparrow}}{v_{F\downarrow}}-1)}{\frac{v_{F\uparrow}}{v_{F\downarrow}}+1}, \tag{42}$$

which has the similar form as equation (34).

4. Results and discussions

There are six calculated figures presented in this paper, in which figures 1–3 are plotted for the system with Rashba SOC in the absence of an external magnetic field, whereas figures 4–6 are plotted for the system with Zeeman splitting in the absence of Rashba SOC.

The dimensionless velocities of the bosonic excitation $u_1(u_2)$ (in units of v_F) as a function of $\delta v_R/v_F$ calculated according to equation (25) in the absence of Zeeman splitting for three different electron–electron interaction strengths of $g = 0.2$ (dotted line), 0.4 (dashed line) and 1 (solid line), respectively, are shown in figure 1. We can see that when the interaction is turned on ($g < 1$) and as $\delta v_R/v_F$ (proportional to the Rashba SOC strength) increases u_1/v_F increases, while u_2/v_F decreases slightly. However, for the stronger interaction the changes of u_1/v_F and u_2/v_F seem less obvious. For a fixed value of $\delta v_R/v_F$, the stronger the interaction is, the larger the velocities of the bosonic excitation $u_1(u_2)$ are. And in the limited case of $\delta v_R/v_F = 0$

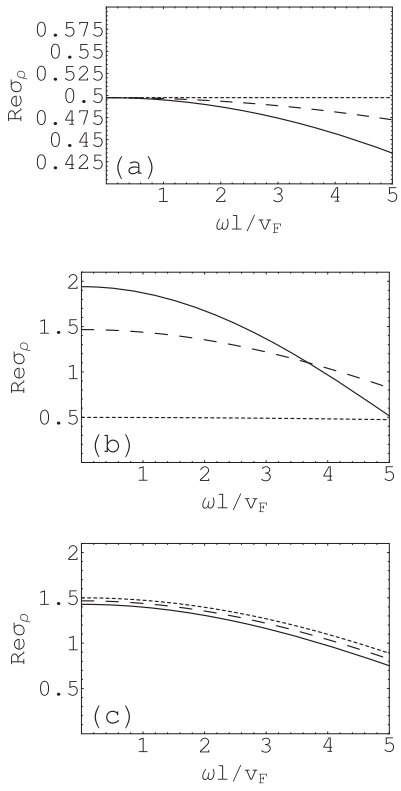

Figure 2. The plotted $\mathrm{Re}\,\sigma_\rho(x,\omega)$ (in units of e^2/h) as a function of $\omega l/v_\mathrm{F}$ in the absence of Zeeman effect (a) with fixed $g = 0.25$ and $\delta v_\mathrm{R}/v_\mathrm{F} = 0.5$ where the solid line is for $\xi = \pm 0.4$, the dashed line for $\xi = \pm 0.25$ and the dotted line for $\xi = 0$; (b) with fixed $\xi = 0.25$ and $\delta v_\mathrm{R}/v_\mathrm{F} = 0.5$ where the solid line is for $g = 1$, the dashed line for $g = 0.75$ and the dotted line for $g = 0.25$; and (c) with fixed $\xi = 0.25$ and $g = 0.75$ where the solid line is for $\delta v_\mathrm{R}/v_\mathrm{F} = 0.75$, the dashed line for $\delta v_\mathrm{R}/v_\mathrm{F} = 0.5$ and the dotted line for $\delta v_\mathrm{R}/v_\mathrm{F} = 0$, respectively.

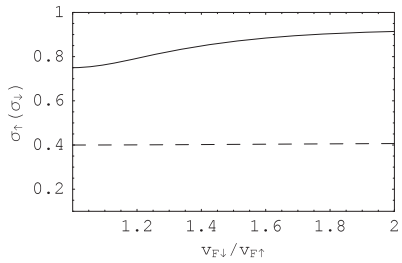

Figure 3. The plotted spin-polarized charge conductivity $\sigma_\uparrow(\sigma_\downarrow)$ (in units of e^2/h) as a function of the ratio $v_{\mathrm{F}\downarrow}/v_{\mathrm{F}\uparrow}$ in the absence of Zeeman effect, where the solid lines correspond to $g = 0.75$ and the dashed lines to $g = 0.4$, respectively.

(i.e., in the absence of SOC), u_1/v_F is equal to $1/g$, whereas u_2/v_F is equal to 1. This is the known result that can be found in [20].

Figure 2 illustrates the real part of the charge conductivity $\mathrm{Re}\,\sigma_\rho(x,\omega)$ (in units of e^2/h) as a function of $\omega l/v_\mathrm{F}$ calculated according to equation (29) in the absence of Zeeman splitting. For the system with fixed $g = 0.25$ and $\delta v_\mathrm{R}/v_\mathrm{F} = 0.5$, figure 2(a) shows the dependence

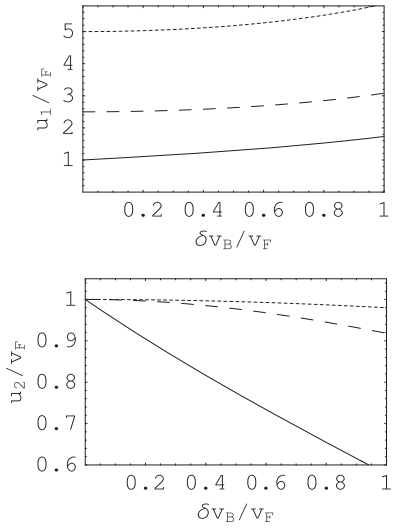

Figure 4. The plotted propagation velocities of the collective modes $u_{1,2}$ (in units of v_F) as a function of the Zeeman strength $\delta v_B/v_F$ in the absence of SOC, where the solid lines correspond to $g = 1$, the dashed lines to $g = 0.4$ and the dotted lines to $g = 0.2$, respectively.

of three different measurement positions $\xi = \pm 0.4$ (solid line), ± 0.25 (dashed line) and 0 (dotted line) on the conductivity, respectively. In the centre of the wire ($\xi = 0$) the conductivity is a constant value regardless of $\omega l/v_F$. However, the further off the wire centre the position, the quicker the change of the conductivity is. Notice that the conductivity only depends on the absolute value $|\xi|$. The influences of the electron–electron interaction g and the Rashba strength $\delta v_R/v_F$ on $\mathrm{Re}\,\sigma_\rho(x,\omega)$ for the system are shown in figures 2(b) and (c), respectively. For the system with fixed $\xi = 0.25$ and $\delta v_R/v_F = 0.5$, figures 2(b) shows the dependence of three different interaction strengths $g = 1$ (solid line), 0.75 (dashed line) and 0.25 (dotted line) on the conductivity, respectively. When the electron–electron interaction parameter g is larger, the variation of $\mathrm{Re}\,\sigma_\rho(x,\omega)$ is faster. If the compositive vibration has a periodicity, then the stronger the interaction is, the longer the period of the oscillation is. The period of the oscillation is the least common multiple of $2\pi u_1/(v_F|\xi|)$ and $2\pi u_2/(v_F|\xi|)$, and the measured position is fixed at $\xi = 0.25$, so the period of the oscillation is totally determined by u_1 and u_2. For the system with fixed $g = 0.75$ and $\xi = 0.25$, figure 2(c) shows the dependence of three different Rashba strengths $\delta v_R/v_F = 0.75$ (solid line), 0.5 (dashed line) and 0 (dotted line) on the conductivity, respectively. Comparing figure 2(c) with 2(b), we can find that the dependence of $\mathrm{Re}\,\sigma_\rho(x,\omega)$ on g at fixed $\delta v_R/v_F$ is very similar to that on $\delta v_R/v_F$ at fixed g, and they exhibit the same tendency as a function of $\omega l/v_F$. But it is obvious that the modification due to the electron–electron interactions is remarkable. Moreover, from figures 2(b) and (c), we can see that the dc ($\omega = 0$) charge conductivities of the system with different electron–electron interactions and Rashba strengths are different constant values, which can be obtained analytically from equation (29) with $\lim_{\omega\to 0}\sigma_\rho(x,\omega) = 2e^2/h[(u_1^2 - v_\sigma^2)v_F/u_1/(u_1^2 - u_2^2) - (u_2^2 - v_\sigma^2)v_F/u_2/(u_1^2 - u_2^2)]$. Here u_1 and u_2 are dependent on both g and α (see figure 1).

In figure 3 we show the dependence of spin-polarized dc conductivity $\sigma_\uparrow(\sigma_\downarrow)$ on the ratio $v_{F\downarrow}/v_{F\uparrow}$ (also proportional to the Rashba SOC strength) in the absence of Zeeman splitting for the two different interaction strengths, where the solid lines correspond to $g = 0.75$ and

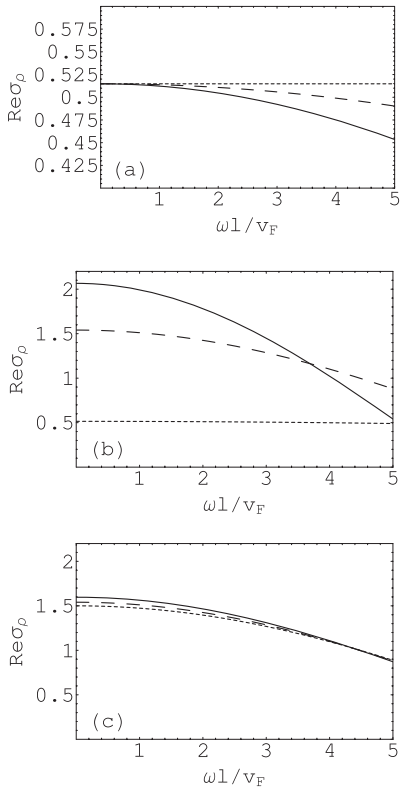

Figure 5. The plotted $\mathrm{Re}\,\sigma_\rho(x,\omega)$ (in units of e^2/h) as a function of $\omega l/v_\mathrm{F}$ in the absence of SOC (a) with fixed $g = 0.25$ and $\delta v_\mathrm{B}/v_\mathrm{F} = 0.5$ where the solid line is for $\xi = \pm 0.4$, the dashed line for $\xi = \pm 0.25$ and the dotted line for $\xi = 0$; (b) with fixed $\xi = 0.25$ and $\delta v_\mathrm{B}/v_\mathrm{F} = 0.5$ where the solid line is for $g = 1$, the dashed line for $g = 0.75$ and the dotted line for $g = 0.25$; and (c) with fixed $\xi = 0.25$ and $g = 0.75$ where the solid line is for $\delta v_\mathrm{B}/v_\mathrm{F} = 0.75$, the dashed line for $\delta v_\mathrm{B}/v_\mathrm{F} = 0.5$ and the dotted line for $\delta v_\mathrm{B}/v_\mathrm{F} = 0$, respectively.

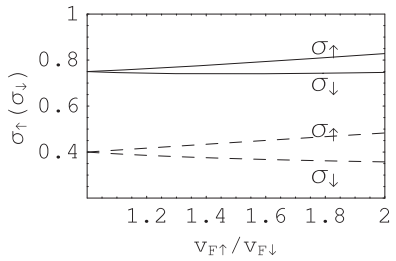

Figure 6. The plotted spin-polarized charge conductivity $\sigma_\uparrow(\sigma_\downarrow)$ (in units of e^2/h) as a function of the ratio $v_{\mathrm{F}\uparrow}/v_{\mathrm{F}\downarrow}$ in the absence of SOC, where the solid lines correspond to $g = 0.75$ and the dashed lines to $g = 0.4$, respectively.

the dashed lines to $g = 0.4$, respectively. The curves for $\sigma_\downarrow$ as a function of $v_{\mathrm{F}\downarrow}/v_{\mathrm{F}\uparrow}$ are the same as those for $\sigma_\uparrow$, and this can be verified from equations (32) and (33). This result implies that the dc conductivities of spin-up and spin-down electrons are degenerate in the absence of a Zeeman effect. From figure 3 we can also see that the spin-polarized conductivities $\sigma_\uparrow(\sigma_\downarrow)$ are connected with the electron–electron interactions for any fixed value of $v_{\mathrm{F}\downarrow}/v_{\mathrm{F}\uparrow}$.

The stronger the interactions the smaller the $\sigma_\uparrow$ ($\sigma_\downarrow$) produced, which shows that the repulsive interaction suppresses the conductivity. Also, the less obvious is the increase of $\sigma_\uparrow$ ($\sigma_\downarrow$) as the increase of ratio $v_{F\downarrow}/v_{F\uparrow}$, which shows that in the case of strong electron–electron interaction the modification of $v_{F\downarrow}/v_{F\uparrow}$ on the conductivity is very little.

Figure 4 shows the dimensionless velocities of the bosonic excitations $u_1(u_2)/v_F$ versus $\delta v_B/v_F$ of the system calculated according to equation (36) in the absence of Rashba SOC for three different interaction strengths of $g = 1$ (solid line), 0.4 (dashed line) and 0.2 (dotted line). We also see that, with the increase of $\delta v_B/v_F$, u_1/v_F increases, while u_2/v_F decreases slightly for all values of $g < 1$. But for the noninteracting case ($g = 1$) u_2/v_F decays more rapidly as $\delta v_B/v_F$ increases, and the stronger the interaction is, the slower the decay of u_2/v_F. Figure 4 is very similar to figure 1, which makes clear that the virtual magnetic field induced by an electric field perpendicular to the 2DEG yields a similar effect on the propagation velocities of the collective modes as the magnetic field applied along the y-direction.

Figure 5 illustrates the real part of the charge conductivity $\mathrm{Re}\,\sigma_\rho(x,\omega)$ (in units of e^2/h) as a function of $\omega l/v_F$ calculated according to equation (38) in the absence of Rashba SOC. For the system with fixed $g = 0.25$ and $\delta v_B/v_F = 0.5$, figure 5(a) shows the dependence of three different measurement positions $\xi = \pm 0.4$ (solid line), ± 0.25 (dashed line) and 0 (dotted line) on the conductivity, respectively. Figure 5(b) shows the dependence of three different interaction strengths $g = 1$ (solid line), 0.75 (dashed line) and 0.25 (dotted line) on the conductivity for the system with fixed $\xi = 0.25$ and $\delta v_B/v_F = 0.5$. And for the system with fixed $g = 0.75$ and $\xi = 0.25$, figure 5(c) shows the dependence of three different magnetic strengths $\delta v_B/v_F = 0.75$ (solid line), 0.5 (dashed line) and 0 (dotted line) on the conductivity, respectively. The variables and the scales in figure 5 are the same as in figure 2 except for replacing $\delta v_R/v_F$ by $\delta v_B/v_F$. Figure 5 is very similar to figure 2. However, from figure 5 we can see that the dc ($\omega = 0$) charge conductivities of the system with different electron–electron interactions or magnetic strengths are different constant values (figures 5(b) and (c)), but with different measurement positions they are the same values (figure 5(a)). This is because $\lim_{\omega\to 0}\sigma_\rho(x,\omega) = 2e^2/h(1/[1-(\delta v_B/(2v_F))^2])[(u_1^2 - v_\sigma^2)v_F/u_1/(u_1^2-u_2^2) - (u_2^2 - v_\sigma^2)v_F/u_2/(u_1^2-u_2^2)]$ where u_1 and u_2 are only dependent on both g and δv_B (see figure 4). These constant values are almost the product of $\mathrm{Re}\,\sigma_\rho(x,\omega = 0)$ in figure 2 and a factor $1/[1-(\delta v_B/2v_F)^2]$, and this is also true in the case of $\omega \neq 0$. Comparing figure 5(c) with 5(b), we can find that the dependence of $\mathrm{Re}\,\sigma_\rho(x,\omega)$ on g at fixed $\delta v_B/v_F$ is very similar to that on $\delta v_B/v_F$ at fixed g, and they exhibit the same tendency as a function of $\omega l/v_F$. But it is obvious that the modification due to the electron–electron interactions is more remarkable, which is the same as the conclusion reached by comparing figure 2(c) with 2(b). Moreover, comparing figure 5(c) with 2(c), we can find that the dependence of $\mathrm{Re}\,\sigma_\rho(x,\omega)$ on $\delta v_B/v_F$ is very similar to that on $\delta v_R/v_F$ in the case of fixed g, and they exhibit the same tendency as a function of $\omega l/v_F$. This means that the effects of Rashba SOC and Zeeman splitting on the conductivity are very similar.

In figure 6 we show how the spin-polarized dc conductivities $\sigma_\uparrow$ and $\sigma_\downarrow$ evolve as the ratio of $v_{F\uparrow}/v_{F\downarrow}$ is varied for the two different interaction strengths, where the solid lines correspond to $g = 0.75$ and the dashed lines to $g = 0.4$, respectively. It is also demonstrated that the increase of ratio $v_{F\uparrow}/v_{F\downarrow}$ pushes $\sigma_\uparrow$ and $\sigma_\downarrow$ away from each other, and one accelerates while the other slows down. This result is in agreement with [9]. In contrast to the Rashba SOC case as shown in figure 3, the ratio of the spin-polarized conductivities $\sigma_\uparrow/\sigma_\downarrow$ is dependent on the electron–electron interactions and the ratio $v_{F\uparrow}/v_{F\downarrow}$. This is because the channel with a larger electron velocity has a larger transmission coefficient for fixed electron–electron interaction strength and $v_{F\downarrow}/v_{F\uparrow}$, and the difference of the transmission coefficient between channels becomes larger with the increase of $v_{F\downarrow}/v_{F\uparrow}$ or of electron–electron interaction strength.

Finally, in II–VI semiconductors the Rashba SOC is expected to be larger than the Dresselhaus coupling, so we can neglect the Dresselhaus SOC [8]. At low temperatures, the 2DEG formed in II–VI semiconductor heterostructures is restricted by a transverse confining potential, so we have a sufficiently long narrow quantum wire. A weak magnetic field B perpendicular to the quantum wire is applied along y-axis, which is turned on or turned off according to the requirement. A longitudinally polarized external electromagnetic field with wavevector along the z-axis irradiates the quantum wire. For the aforementioned reasons, the present experimental condition may be reachable [2–4]. Furthermore, in this article we have only considered the case of infinite-length LL. This situation is important for a simple theoretical understanding, although it may be relevant to experiments where the leads always dominate the results. The conductivity of a finite-length LL coupled to leads may have different frequency and amplitude dependence on the physical parameters of the system due to the Andreev-type reflections [19]. The detailed calculation and discussion for the important role of the Fermi liquid leads on the conductivity of the system will be given in our next work.

5. Conclusion

In conclusion, using a straightforward approach we have investigated theoretically the transport properties through an interacting quantum wire in the presence of both Rashba SOC and Zeeman splitting simultaneously in the LL regime. Using the bosonization technique, the equations of motion of bosonic phase fields for the system with a longitudinal electric field is established, and the solution is obtained by introducing a Fourier transformation in which the spin and charge degrees of freedom are completely coupled and characterized by four new different velocities. Within the linear response theory, it is found that the ac conductivity of an LL wire in the presence of Rashba SOC and Zeeman splitting is generally an oscillation function of the interaction strength g, Rashba SOC strength α, Zeeman interaction strength B and the driving frequency ω as well as the measurement position x in the wire.

For an LL wire with only Rashba SOC, the real part of the conductivity $\mathrm{Re}\,\sigma_\rho$ as a function of the electron–electron interaction or Rashba SOC strength exhibits similar decay tendencies with the increase of frequency $\omega l/v_\mathrm{F}$. But the modification due to the electron–electron interactions is more remarkable than that due to Rashba SOC. On the other hand, for a LL wire only with only Zeeman splitting, $\mathrm{Re}\,\sigma_\rho$ is a function of the frequency $\omega l/v_\mathrm{F}$; the same curves hold if one replaces $\delta v_\mathrm{R}/v_\mathrm{F}$ by $\delta v_\mathrm{B}/v_\mathrm{F}$, but one has to multiply all values of $\mathrm{Re}\,\sigma_\rho$ by a factor of $1/[1-(\delta v_\mathrm{B}/2v_\mathrm{F})^2]$.

For an LL with only Rashba SOC, when we study how $\sigma_\uparrow(\sigma_\downarrow)$ evolve as the ratio $v_{\mathrm{F}\downarrow}/v_{\mathrm{F}\uparrow}$ is varied, we find that the curves for $\sigma_\downarrow$ as a function of $v_{\mathrm{F}\downarrow}/v_{\mathrm{F}\uparrow}$ are the same as those for $\sigma_\uparrow$. But for an LL with only Zeeman splitting, we find that the increase of the ratio $v_{\mathrm{F}\uparrow}/v_{\mathrm{F}\downarrow}$ pushes $\sigma_\uparrow$ and $\sigma_\downarrow$ away from each other, which is consistent with the result of the previous studies [9] for the same system. In contrast to the SOC case, the ratio of the spin-polarized conductivities $\sigma_\uparrow/\sigma_\downarrow$ is dependent on the electron–electron interactions.

Further investigations are worth being done for the higher conductivity corrections, in the presence of impurity, or with realistic Coulomb interactions.

Acknowledgments

This work was supported by National Natural Science Foundation of China (Grant No. 10574042), Specialized Research Fund for the Doctoral Program of Higher Education of China (Grant No. 20060542002) and Hunan Provincial Natural Science Foundation of China (Grant No. 06JJ2097).

References

[1] Voit J 1995 *Rep. Prog. Phys.* **58** 977
[2] Yacoby A, Stormer H L, Wingreen N S, Pfeiffer L N, Baldwin K W and West K W 1996 *Phys. Rev. Lett.* **77** 4612
[3] Bockrath M, Cobden D H, Lu J, Rinzler A G, Smalley R E, Balents L and McEuen P L 1999 *Nature* **397** 598
[4] Chang A M, Pfeiffer L N and West K W 1996 *Phys. Rev. Lett.* **77** 2538
[5] Wolf S A, Awschalom D D, Buhrman R A, Daughton J M, von Molnár S, Roukes M L, Chtchelkanova A Y and Treger D M 2001 *Science* **294** 1488
[6] Bychkov Y A and Rashba E I 1984 *J. Phys. C: Solid State Phys.* **17** 6039
[7] Dresselhaus G 1955 *Phys. Rev.* **100** 580
[8] Nitta J, Akazaki T, Takayanagi H and Enoki T 1997 *Phys. Rev. Lett.* **78** 1335
[9] Kimura T, Kuroki K and Aoki H 1996 *Phys. Rev.* B **53** 9572
[10] Moroz A V, Samokhin K V and Barnes C H W 2000 *Phys. Rev. Lett.* **84** 4164
Moroz A V, Samokhin K V and Barnes C H W 2000 *Phys. Rev.* B **62** 16900
[11] Iucci A 2003 *Phys. Rev.* B **68** 075107
[12] Gritsev V, Japaridze G, Pletyukhov M and Baeriswyl D 2005 *Phys. Rev. Lett.* **94** 137207
[13] Hankiewicz E M and Vignale G 2006 *Phys. Rev.* B **73** 115339
[14] Yu Y, Wen Y, Li J, Su Z and Chui S T 2004 *Phys. Rev.* B **69** 153307
[15] Devillard P, Crepieux A, Imura K I and Martin T 2005 *Phys. Rev.* B **72** R041309
[16] Ponomarenko V V 1996 *Phys. Rev.* B **54** 10328
Sharma P and Chamon C 2003 *Phys. Rev.* B **68** 035321
Feldman D E and Gefen Y 2003 *Phys. Rev.* B **67** 115337
Cheng F and Zhou G H 2006 *Phys. Rev.* B **73** 125335
[17] Sassetti M and Kramer B 1996 *Phys. Rev.* B **54** R5203
[18] Cuniberti G, Sassetti M and Kramer B 1998 *Phys. Rev.* B **57** 1515
Fechner A, Sassetti M, Kramer B and Galleani d'Agliano E 2001 *Phys. Rev.* B **64** 195315
[19] Maslov D L and Stone M 1995 *Phys. Rev.* B **52** R5539
Ponomarenko V V 1995 *Phys. Rev.* B **52** R8666
Maslov D L 1995 *Phys. Rev.* B **52** R14368
Safi I and Schulz H J 1995 *Phys. Rev.* B **52** R17040
Sandler N P, Chaman C C and Frakin E 1998 *Phys. Rev.* B **57** 12324
Dolcini F, Trauzettel B, Safi I and Grabert H 2005 *Phys. Rev.* B **71** 165309
Janzen K, Meden V and Schönhammer K 2006 *Phys. Rev.* B **74** 085301
[20] Gogolin A O, Nersesyan A A and Tsvelik A M 1998 *Bosonization and Strongly Correlated Systems* (Cambridge: Cambridge University Press)